

THE LOS ALAMOS FREE-ELECTRON LASER*

J. M. Watson, AT-7, MS H825
Los Alamos National Laboratory, Los Alamos, NM 87545 USA

Summary

During the past year the Los Alamos free-electron laser (FEL) oscillator has demonstrated high peak and average power (10 MW and 6 kW), broad-wavelength tunability (9–35 μm), and near-ideal optical quality (0.9 Strehl ratio). An electron energy-extraction efficiency of 1% was measured. The predicted production of synchrotron sidebands also was observed in the broadened optical spectrum. As shorter wavelengths and higher powers are pursued, higher currents with improved beam quality will be required. Advanced injectors and energy-recovery systems are being developed to meet these demands.

Introduction

Free-electron lasers are being actively developed at many Laboratories because of several highly desirable properties. These lasers span the wavelength range from centimeters to tenths of micrometers and should be continuously tunable over an order of magnitude by varying the electron beam energy, the wiggler wavelength, or both. Recent experiments indicate that the optical quality is excellent at modest power levels. FELs are scalable to high average power because the lasing medium is the electron beam itself and it is removed from the cavity at nearly the speed of light, thus avoiding the cooling problems associated with using solid or gaseous lasing media. Finally, it appears that FELs can be quite efficient through the use of tapered wigglers and the recovery of most of the kinetic energy left in the beam.

The basic components of an FEL are an electron beam, an external oscillatory field, and a radiation field. The external oscillatory field causes the moving electrons to oscillate ("wobble") transversely so that the transverse electric field of the imposed photons can bunch and decelerate the electrons. The deceleration energy of the electrons appears as a coherent enhancement of the radiation field.

FELs are configured as amplifiers or oscillators. An amplifier increases the power of an external radiation source during a single pass through the wiggler. This configuration is best suited to the high-gain FELs operating in the Raman (intense current) regime. An FEL oscillator employs an optical resonator around the wiggler that allows the radiation field to build up with time through many synchronous passes with multiple electron pulses through the wiggler. If the pulse train is long enough and the small-signal gain (SSG) is adequate, an FEL oscillator should start up from spontaneous emission without an externally injected radiation field.

The remainder of this paper will concentrate on short-wavelength ($\leq 10\text{-}\mu\text{m}$) FEL oscillators operating in the Compton regime where there has been substantial progress lately. A recent, excellent review¹ by Sprangle and Coffey lists most of the FEL experiments and their wide range of parameters. The status of the rf-linac-driven FELs has been reviewed recently by Brau.²

In Fig. 1 we show the basic elements of a Compton-regime FEL oscillator, which consists of a pulsed beam of relativistic electrons from an rf linac directed through a static, periodic, transverse magnetic field

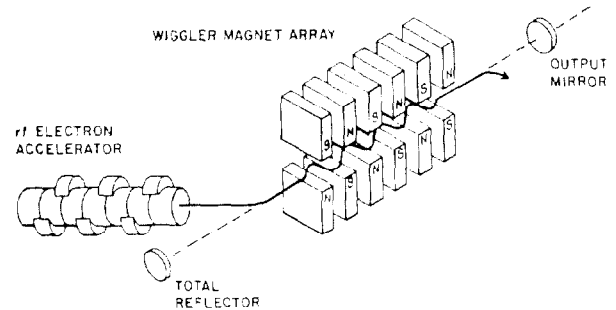


Fig. 1. The basic elements of a Compton-regime FEL oscillator: relativistic electron beam, magnetic wiggler, and optical resonator.

(called a wiggler), and an optical resonator with one mirror slightly transmitting for output coupling. The electrons oscillate transversely and emit polarized radiation at a wavelength λ_s determined by the resonance condition,

$$\lambda_s = \frac{\lambda_w}{2\gamma^2} (1 + K^2/2) \quad (1)$$

where λ_w is the wiggler period, γ is the electron energy in units of its rest mass, and $K = e\lambda_w B/2\pi mc^2$ with B being the peak magnetic field at the wiggler mid-plane. The emission from the initial electron pulses passing through the wiggler is primarily spontaneous. The precisely spaced mirrors provide a round-trip time for the light, which matches the period of the electron bunches. As the captured radiation field increases, the transverse electric field of the light causes longitudinal bunching on an optical-wavelength spatial scale. When the average electron energy is above the resonant energy defined in Eq. (1), the radiation field causes a net deceleration accompanied by "stimulated emission." If the optical gain of the wiggler at low power levels exceeds the mirror and diffraction losses, there will be a rapid build-up of this stimulated radiation until the power losses (including outcoupling) equal the power produced.

FEL Oscillator Experiments

Since the first operation of an FEL oscillator at Stanford University in 1977,³ FEL theory and simulations have advanced substantially. The introduction of an accelerator-based description, which led to the tapered wiggler,⁴ is resulting in higher efficiencies. FEL amplifier experiments at Los Alamos⁵ and Math Sciences/Boeing⁶ have demonstrated 4% efficiencies.

In 1983 and 1984, three oscillators were demonstrated as shown in Table I. These oscillators used a conventional linac, a superconducting (sc) linac, a storage ring, and spanned a wide range of powers and wavelengths.

The University of Paris/Stanford experiment at Orsay represents the first operation of a visible wavelength FEL on a storage ring,⁷ which used a 1.3-m, permanent-magnet optical-klystron wiggler (containing magnetic bunching). With a 50-mA ring current, a net gain per pass of ~ 0.001 was achieved. The oscillations grew for 200 μs and then stabilized at 2-kW intracavity peak power during the 1-ns electron

*Work performed under the auspices of the US Dept. of Energy and supported by the US Dept. of Defense Ballistic Missile Defense Organization.

TABLE I
SUMMARY OF SHORT-WAVELENGTH FEL OSCILLATORS

Year	Institution	Accelerator	Beam Energy (MeV)	Wavelength	Peak Power	Average Power ^a
1977	Stanford*	sc linac	43	3.4 μm	135 kW	5 W
1983	U Paris/Stanford*	ACO	160	640-655 nm	60 mW	75 μW
1983	TRW/Stanford*	sc linac	66	1.6 μm	1 MW	80 W
1984	Los Alamos*	rf linac	23-11.5	9-35 μm	10 MW	6 kW

^aAverage power during each beam macropulse.

bunches. The primary problem encountered was the degradation of the mirror coatings by the ultraviolet radiation from the ring and wiggler. With such a small gain, practically any degradation could prevent oscillation build-up.

The TRW/Stanford experiment was performed at Stanford on the superconducting linac,⁸ which represents the first oscillator with a tapered wiggler. The accelerator was operated at 66 MeV with peak currents from 0.5 to 2.5 A with very low emittance and small energy spread. A 5.4-m permanent-magnet wiggler was used that contained two 0.5-m constant-period sections, a magnetic bunching section, and a 3.2-m adjustable tapered section. With a 1% taper in γ , a 7% gain per pass was achieved, reaching saturation in 25 μs . The peak cavity power was 1.2 MW and the average output power was 80 W at 1.6 μm . The efficiency obtained was 1.1%, which was a factor of 3 greater than the performance of the wiggler with no taper.

Los Alamos FEL Oscillator Experiment (OSX)

The schematic layout of the Los Alamos FEL oscillator⁹ is shown in Fig. 2, and the typical 10- μm operating parameters are listed in Table II. The electron gun produces a train of 2000 micropulses, spaced 46 ns apart, for a macropulse of 100 μs . These micropulses are bunched and accelerated to ~ 21 MeV. The train of high-current pulses then passes through the wiggler, generating spontaneous emission followed by stimulated emission, which grows exponentially to a saturated level of optical power.

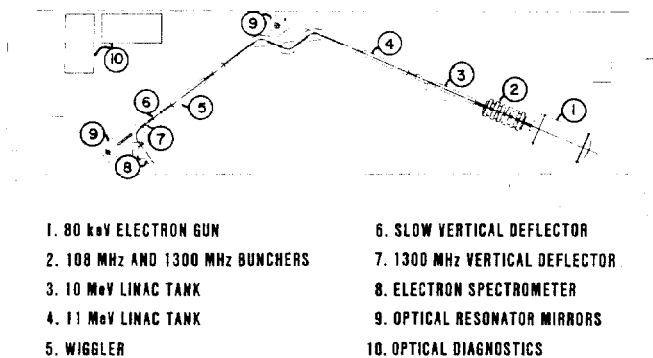


Fig. 2. FEL block diagram.

The mirrors of the optical resonator were curved for a stable, fundamental mode of the correct size to maximize the wiggler's gain. The mirrors were composed of multiple dielectric layers deposited on ZnSe substrates transparent to visible light. This combination allowed use of a He-Ne laser for mirror alignment and alignment of the electron beam with the resonator. The mirrors were remotely tilted for optimum alignment, and the end mirror was translated longitudinally to achieve the correct spacing. A separate He-Ne interferometer monitored the mirror spacing continuously.

TABLE II
FEL OSCILLATOR PARAMETERS

Electron Beam	
Electron energy	21 MeV
Accelerator frequency	1.3 GHz
Micropulse width	35 ps
Peak current	40 A
Micropulse repetition time	46.2 ns
Macropulse length	100 μs
Energy spread	2% (FWHM)
Emittance	2.5 $\mu\text{m-mrad}$
Diameter at waist	2.0 mm
Wiggler	
Length	100 cm
Period	2.73 cm
Number of periods	37
Gap between magnets	0.88 cm
Field strength	0.31 T
Optical	
Cavity length	6.92 m
Rayleigh range	63.2 cm
Diameter at waist	2.9 mm
Wavelength	10.5 μm
Round-trip losses	6.5%
Output coupler	5.1%
Small-signal energy gain	40%
Average output power	6 kW
Peak output power	10 MW
Peak intracavity power	200 MW
Extraction efficiency	1%
Cavity tuning range	60 μm

Small-Signal Gain

The SSG was routinely measured at the beginning of each lasing experiment using a Hg:Ge photodetector. The SSG depended strongly on the peak electron current, and net values up to 60% were recorded for peak currents up to 50 A. The current required to reach the lasing threshold was 7 A. Figure 3 shows an example of the exponential rise with a 34% SSG starting from incoherent spontaneous emission. The total radiation growth from spontaneous emission to saturation ranged between six to seven orders of magnitude.

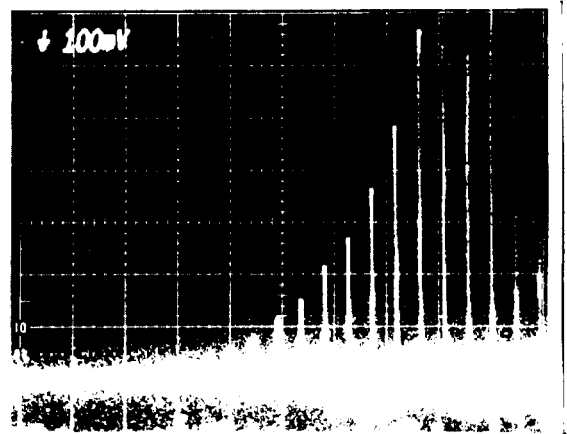


Fig. 3. Exponential rise of the lasing micropulse energy from spontaneous emission en route to saturation at the start of the electron-beam macropulse. A net small-signal energy gain of 34% per cavity round trip is represented.

Output Power and Efficiency

The total energy produced in a train of optical pulses within a macropulse was measured with an energy calorimeter for each shot as shown in Fig. 4. The cavity length and axis were tuned for maximum output and minimum optical losses as determined by the decay time

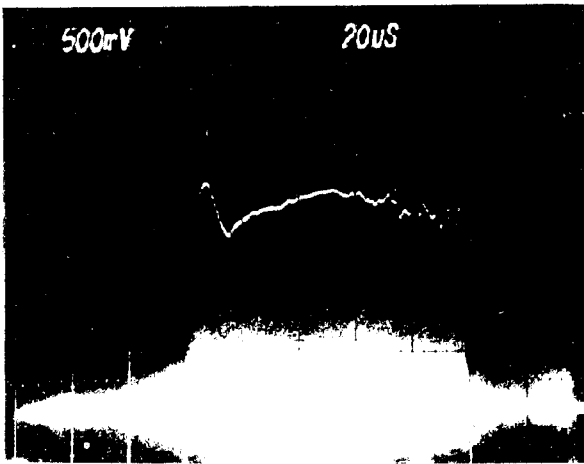


Fig. 4. Output power for strongly saturated lasing with 40-A peak current and zero cavity-length detuning. The temporal envelope follows the current macropulse with minimal instability caused by energy variations in the electron beam.

of the optical signal at the end of the electron current macropulse. Maximum output was produced with maximum peak electron current and large output coupling from the resonator. With a 40-A peak current and a 5% output coupler, an output energy in excess of 500 mJ was produced within a 90- μ s pulse train. At 1 pps, that corresponds to 6 kW of average power over the macropulse, or 0.5-W average over an hour. Measurements of the temporal shape of individual electron micropulses yielded a Lorentzian shape with FWHM of 35 ± 5 ps. Assuming a 30-ps optical pulse width during the high-power tests (low-level beam current in the temporal wings did not take part in the lasing), a peak output power of 10 MW was obtained. This peak power translates to 200 MW of circulating power inside the resonator when the 5% outcoupling measurements indicated a maximum energy-extraction efficiency of 0.75%.

The extraction efficiency can also be obtained by comparing the energy distribution at a certain time during lasing with the distribution at the corresponding time in the macropulse without lasing. The energy spectra from a number of different macropulses with and without lasing have been plotted for 40-A peak currents in Fig. 5. For this measurement, the low-energy tail of the electron distribution was removed by a scraper in the 60° achromatic bends. The energy change from the nonlasing to the lasing condition, as well as the reproducibility of the data, are evident. The measured extraction efficiency ($1.0 \pm 0.2\%$) is determined from the difference in average energy of these two curves.

Synchrotron Sidebands

Special emphasis was given to the measurement and interpretation of the optical spectra. As predicted by Kroll, et al.,¹⁰ the spectra generally did not have a single, narrow peak, but gave abundant evidence of synchrotron sideband generation observed here for the first time. Previous spectral measurements in the Stanford University/TRW FEL experiments did not reveal features associated with this instability, presumably because of their short 3-ps micropulse. In this experiment when the laser was oscillating near threshold, either by cavity detuning or reduced electron current, a single spectral peak was observed. The minimum FWHM integrated over the macropulse measured was 0.3%, which is a factor of 6 broader than the Fourier transform of the 30-ps optical pulse. It is possible that some of the width was due to variation of the wavelength caused

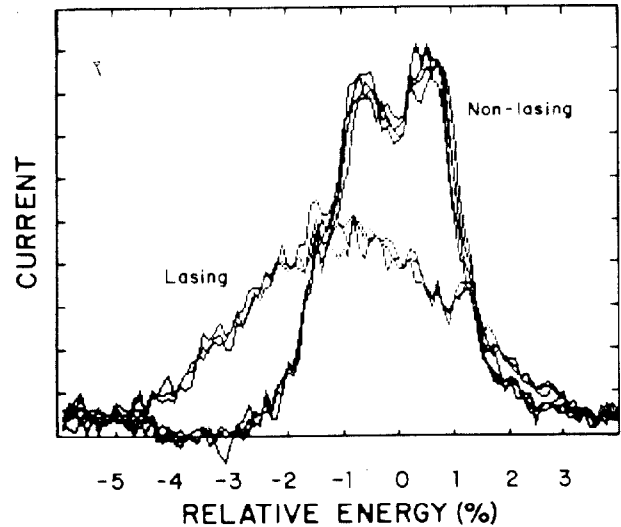


Fig. 5. Energy distributions with and without lasing averaged over many micropulses. Six spectra of each kind are superimposed.

by electron-energy changes. At higher powers, a richly structured multiple-peak spectrum was usually observed. The total FWHM of the spectra often reached 4%. Significant variations in the relative heights of the several peaks often occurred, presumably because of electron current variations.

Wavelength Tuning

At the end of this year-long series of oscillator experiments confined to the 9- to 11- μ m reflectance band of the multilayer reflectors, a special experiment was conducted to demonstrate the broad-wavelength tunability inherent to FEL devices. First, the multilayer reflectors were replaced by uncoated copper mirrors, with the output mirror having a 1.8-mm-diam axial hole to couple out the optical radiation (2.4% transmission at 10 μ m) extracted from the electron beam. Then, by varying the electron energy from 23 to 11.5 MeV, the laser radiation was tuned continuously from 9 to 35 μ m, a factor of 4. As the wavelength increased, the total cavity losses declined because of reduced transmission through the output coupler, which is consistent with the larger divergence and beam diameter expected. Also, over the range in which the fundamental lasing wavelength was detectable, the SSG was measured and was found to increase with wavelength as predicted by FEL theory. With more experience in properly bunching and transporting a lower energy electron beam through the 60° bending magnets, the tuning range of this system probably could be extended to wavelengths approaching 100 μ m.

Spatial Beam Quality

Many applications of high-power lasers require high intensities on a target surface or throughout a volume of material. It is therefore highly desirable that all of a laser's output power be focusable to the smallest possible diameter. Theoretically, this is realizable with a diffraction-limited beam having a Gaussian intensity profile with no phase distortions. According to the theoretical analysis of Quimby and Slater¹¹ and Bhowmik and Cover,¹² the FEL has the potential for diffraction-limited output with only minimal intra-cavity aperturing. Indeed, with a low-current electron beam with extremely small emittance, the Stanford University/TRW FEL has demonstrated excellent beam quality, albeit at modest optical power levels.¹³

Measurement of the spatial beam quality of a high-power FEL oscillator, driven by high-current electron pulses with correspondingly larger beam emittance, was one of the major goals of the Los Alamos FEL experiment. An extensive series of tests yielded a quantitative measure of the beam quality in the far fields after a 1-m focal-length lens. No apertures, other than the mirror mounts and the 6.6-mm-diam opening at the entrance of the wiggler, were used for mode control. The quantitative measure of beam quality was the Strehl ratio of axial intensities. A Strehl ratio of unity indicates a perfect, unaberrated beam of Gaussian intensity profile. Such would correspond to the lowest order mode of the optical resonator. A series of measurements was made of the beam spot size as a function of distance from the lens on both sides of the focus. An analysis of a least-squares fit to the beam radii versus distance from the focal plane yielded a Strehl ratio value of 0.9. This very large value is consistent with the close resemblance of the focused beam to a Gaussian. The small deviation from a unity Strehl ratio, corresponding to a net phase distortion of $\lambda/22$, could have been due to interaction with the electrons or imperfections in the cavity mirrors or external optics.

Los Alamos FEL Oscillator Improvements

Higher peak currents, improved electron beam quality, and greater overall efficiency are primary goals of the Los Alamos FEL program. The oscillator is now undergoing extensive changes to accomplish these goals. The changes include an extensively modified injector, an rf energy-recovery system, and development of laser-illuminated photocathode injectors.

Energy-Recovery Experiment (ERX)

The Los Alamos FEL will soon begin a series of experiments to demonstrate improved extraction efficiencies and enhanced average power. Higher extraction efficiencies will be accomplished by injector improvements that should produce peak electron currents exceeding 100 A with improved emittance. Multipactoring in one subharmonic buncher and the lack of solenoidal fields over the first linac tank have limited the peak currents to 50 A with an emittance of $2.5 \pi \cdot \text{mm} \cdot \text{mrad}$. Simulations of a modified injector system indicate that peak currents of over 100 A with $1 \pi \cdot \text{mm} \cdot \text{mrad}$ should be achieved. An important feature of the modified design is the proximity of the fundamental buncher to the linac. Because the gain of the FEL is linearly proportional to the current, the performance should be improved significantly.

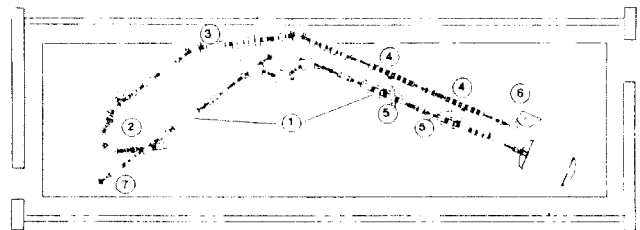
After passing through the FEL, the electron beam will have more than 90% of its original power and will still have its microbunch structure. The mix of particles that were, and were not, captured by the photons' deceleration bucket introduces several per cent of energy spread. This spread makes the beam unsuitable for recirculation through the wiggler. However, the overall efficiency of the FEL can be greatly enhanced through recovery of most of the power in the residual electron beam. It appears that the most efficient method of recovering the kinetic energy of the beam in a FEL in this regime is through deceleration in rf-excited linear accelerator structures. The kinetic energy is thereby converted into rf power that is used to accelerate new beam. A conversion efficiency greater than 99% appears possible. Energy recovery in an electrostatic accelerator used on the FEL at Santa Barbara already has been accomplished.¹⁴

The ERX will use decelerator structures that are separate from the accelerator to provide maximum experimental flexibility. Variable rf bridge couplers will facilitate the rf power transfer over a wide

range of deceleration values.¹⁵ The ERX parameters are listed in Table III and its layout is shown schematically in Fig. 6. The major new systems added to the oscillator experiment are an isochronous return beamline, two side-coupled decelerator tanks, and two variable bridge couplers. Each accelerator/decelerator pair is excited by a common klystron with gradient ratios determined by the bridge coupler. The 180° bend is mounted on a translation table to adjust the beam path for the proper decelerating phase angle.

TABLE III
IMPROVED OPERATING PARAMETERS IN ERX

	Oscillator Experiment	ERX
Macropulse Duration (μs)	100	100
Micropulse Repetition Rate (MHz)	21.7	108.3
Peak Current (A)	50	100
Average Current (A)	0.05	0.30
Emittance ($\pi \cdot \text{mm} \cdot \text{mrad}$)	2.5	1
Accelerator Efficiency	0.36	0.74
Deceleration (MeV)	0	18
Copper Losses (MW)	2.7	4.5
Beam Power (MW)	1.0	6.0
Recovered Power (MW)	0	4.6
Efficiency Improvement	1	1.5
Optical Power (kW)	6	>50



- 1 OSX ACCELERATOR AND FEL OPERATING AT FIVE-FOLD INCREASE IN AVERAGE CURRENT
- 2 ISOCHRONOUS 180° BEND ON TRANSLATION TABLE
- 3 ISOCHRONOUS 60° BEND
- 4 TWO 1.8-m DECELERATOR (ENERGY-RECOVERY) SECTIONS
- 5 TWO VARIABLE rf BRIDGE COUPLERS
- 6 BEAM DUMP FOR 2- TO 3-MeV BEAM
- 7 20-MeV DIAGNOSTICS

Fig. 6. Layout of FEL oscillator with energy recovery.

The injector will be operated at 108 MHz in the second phase of ERX to improve the overall efficiency enhancement by nearly 50%. One of the most important considerations in achieving large enhancements is attaining high average beam power relative to the copper losses of the structures. It is possible to use the accelerator itself simultaneously to decelerate electrons and thereby eliminate the losses associated with a separate decelerator. However, this method is less flexible and is more prone to break-up instabilities at high electron-beam currents.

Advanced Injectors

Most of the emittance growth in conventional electron linacs occurs during the bunching and acceleration to relativistic energy (a few MeV). For bunches with several nanocoulombs, the growth in the normalized transverse emittance usually is more than an order of magnitude above the gun emittance. High-current optical-wavelength FELs will require normalized emittances smaller than $40 \pi \cdot \text{mm} \cdot \text{mrad}$ --most of the conventional injector emittance growth must be avoided.

At Los Alamos, an experimental program is under way to develop injectors with high current-density photocathodes that can be operated in high-field rf cavities

and frontally illuminated with mode-locked short-pulse lasers.¹⁶ The already short bunches will be accelerated quickly in the rf cavity, which is the first cell of the injector. Photocathodes such as GaAs and Cs₃Sb are being investigated and are capable of current densities exceeding 250 A/cm² with modest laser illumination.¹⁷ Present simulations indicate that 1-A average current with a normalized emittance less than 20 $\mu\text{m}\cdot\text{mrad}$ may be achieved with this type of injector. The demonstration of a reliable injector of this type is expected within the next two years at Los Alamos.

Conclusions

The Los Alamos experiments have demonstrated that FELs are capable of their expected attributes: good efficiency, broad wavelength tunability, excellent optical quality, and high peak power. During the next year, the improvements to the Los Alamos FEL should result in even better and more reliable performance, as well as demonstrating a technique for achieving very high efficiencies in high average-power free-electron lasers.

Acknowledgments

The Los Alamos FEL program was conceived by and is carried out under the general leadership of C. A. Brau. The operation of the FEL oscillator experiments is directed by R. W. Warren. The optical measurements are the responsibility of B. E. Newnam. Subsystems contributions are made by the following: injectors, J. S. Fraser and L. M. Young; accelerators, W. E. Stein, L. M. Young, and G. Spalek; rf systems, M. T. Lynch, W. E. Stein, C. Friedrichs, and P. J. Tallerico; wiggler, R. W. Warren; electron diagnostics, J. S. Fraser, R. L. Sheffield, W. E. Stein, and A. H. Lumpkin; optics, B. E. Newnam, J. E. Sollid, and T. A. Swann; and theoretical support, R. K. Cooper and J. C. Goldstein. The operating support of O. R. Norris, T. O. Gibson, and M. C. Whitehead is crucial. The mechanical support is directed by B. M. Campbell, P. M. Giles, L. D. Hansborough, D. J. Liska, F. E. Sigler, and R. L. Stockley. The electronic support is led by D. C. Stephens and J. G. Winston. The concerted efforts by this team are gratefully acknowledged by the author who is also thankful for their contributions to this status report.

References

1. P. Sprangle and T. Coffey, "New Sources of High-Power Coherent Radiation," *Physics Today*, March 1984, 44.
2. C. A. Brau, "Free-Electron Lasers Driven by RF Linacs," *IEEE J. Quantum Electron.*, to be published, June 1985.
3. D. A. G. Deacon, L. R. Elias, J. M. J. Madey, G. J. Romian, H. A. Schwettman, and T. I. Smith, *Phys. Rev. Lett.*, **38** (1977), 892.
4. N. M. Kroll, P. L. Morton, M. N. Rosenbluth, "Variable Parameter Free-Electron Laser," *Free-Electron Generators of Coherent Radiation*, Physics of Quantum Electronics series, (Addison-Wesley), **1** (1980), 89.
5. R. W. Warren, B. E. Newnam, J. G. Winston, W. E. Stein, L. M. Young, and C. A. Brau, "Results of the Los Alamos Free-Electron Laser Experiment," *IEEE J. Quantum Electron.*, **QE-19** (1983), 391.
6. J. M. Slater, J. Adamski, D. C. Quimby, T. L. Churchill, L. Y. Nelson, and R. E. Center, "Electron Spectrum Measurements for a Tapered Wiggler Free-Electron Laser," *IEEE J. Quantum Electron.*, **QE-19** (1983), 374.
7. M. Billardon, P. Elleaume, J. M. Ortega, C. Bazin, M. Bergher, Y. Petroff, M. Velghe, D. A. G. Deacon, K. E. Robinson, and J. M. J. Madey, "First Operation of a Storage Ring Free-Electron Laser," *Free-Electron Generators of Coherent Radiation*, C. A. Brau, S. F. Jacobs, and M. O. Scully, Eds., *Proc. SPIE 453* (1984), 52; also *Phys. Rev. Lett.*, **51** (1983), 1652.
8. J. A. Edighoffer, G. R. Neil, C. E. Hess, T. I. Smith, S. W. Fornaca, and H. A. Schwettman, "Variable-Wiggler Free-Electron Laser Oscillation," *Phys. Rev. Lett.*, **52** (1984), 344.
9. B. E. Newnam, R. W. Warren, R. L. Sheffield, W. E. Stein, M. T. Lynch, J. S. Fraser, J. C. Goldstein, J. E. Sollid, T. A. Swann, J. M. Watson, and C. A. Brau, "Optical Performance of the Los Alamos Free-Electron Laser," *IEEE J. Quantum Electron.*, to be published, June 1985.
10. N. M. Kroll, P. L. Morton, and P. L. Rosenbluth, "Free-Electron Lasers with Variable Parameter Wigglers," *IEEE J. Quantum Electron.*, **QE-17** (1981), 1436.
11. D. C. Quimby and J. Slater, "Mode Structure Of A Tapered-Wiggler Free-Electron Laser Stable Oscillator," *IEEE J. Quantum Electron.*, **QE-19** (1983), 800.
12. A. Bhowmik and R. A. Cover, "Misalignments, Mode Distortions and Higher Order Modes In Free-Electron Laser Oscillators," Presented at Int. Conf. On Lasers '84, San Francisco, California, November 26-30, 1984.
13. G. R. Neil, J. A. Edighoffer, and S. Fornaca, "Measurements of Optical Beam Quality in an FEL," In *Free-Electron Generators of Coherent Radiation*, *Proc. SPIE 453* (1984), 114.
14. L. R. Elias, "Status Report of the UCSB FEL Research Effort," *Proc. SPIE 453* (1984), 52; also *Phys. Rev. Lett.*, **51** (1983), 1652.
15. G. Spalek, J. H. Billen, J. A. Garcia, P. M. Giles, L. D. Hansborough, D. E. McMurry, and S. B. Stevens, "The Free-Electron Laser Variable Bridge Coupler," these proceedings.
16. J. S. Fraser, R. L. Sheffield, E. R. Gray, and G. W. Rodenz, "High-Brightness Photoemitter Injector for Electron Accelerators," these proceedings.
17. C. Lee, P. Dettinger, E. Pugh, R. Klinkowstein, J. Jacob, J. S. Fraser, and R. L. Sheffield, "Electron Emission of Over 200 A/cm² from a Pulsed-Laser Irradiated Photocathode," these proceedings.